 doi:10.1111/j.1525-1314.2005.00619.x

Ultrahigh-pressure metamorphism and exhumation of garnet peridotite in Pohorje, Eastern Alps

M. JANÁK[1], N. FROITZHEIM[2], M. VRABEC[3], E. J. KROGH RAVNA[4] AND J. C. M. De HOOG[5]
[1]Geological Institute, Slovak Academy of Sciences, Dúbravská 9, P.O. Box 106, 840 05 Bratislava 45, Slovak Republic (marian.janak@savba.sk)
[2]Geologisches Institut, Universität Bonn, Nussallee 8, D-53115 Bonn, Germany
[3]Department of Geology, University of Ljubljana, Aškerčeva 12, 1000 Ljubljana, Slovenia
[4]Department of Geology, University of Tromsø, N-9037 Tromsø, Norway
[5]Institute of Earth Sciences, Göteborg University, 405 30 Göteborg, Sweden

ABSTRACT New evidence for ultrahigh-pressure metamorphism (UHPM) in the Eastern Alps is reported from garnet-bearing ultramafic rocks from the Pohorje Mountains in Slovenia. The garnet peridotites are closely associated with UHP kyanite eclogites. These rocks belong to the Lower Central Austroalpine basement unit of the Eastern Alps, exposed in the proximity of the Periadriatic fault. Ultramafic rocks have experienced a complex metamorphic history. On the basis of petrochemical data, garnet peridotites could have been derived from depleted mantle rocks that were subsequently metasomatized by melts and/or fluids either in the plagioclase-peridotite or the spinel-peridotite field. At least four stages of recrystallization have been identified in the garnet peridotites based on an analysis of reaction textures and mineral compositions. Stage I was most probably a spinel peridotite stage, as inferred from the presence of chromian spinel and aluminous pyroxenes. Stage II is a UHPM stage defined by the assemblage garnet + olivine + low-Al orthopyroxene + clinopyroxene + Cr-spinel. Garnet formed as exsolutions from clinopyroxene, coronas around Cr-spinel, and porphyroblasts. Stage III is a decompression stage, manifested by the formation of kelyphitic rims of high-Al orthopyroxene, aluminous spinel, diopside and pargasitic hornblende replacing garnet. Stage IV is represented by the formation of tremolitic amphibole, chlorite, serpentine and talc. Geothermobarometric calculations using (i) garnet-olivine and garnet-orthopyroxene Fe-Mg exchange thermometers and (ii) the Al-in-orthopyroxene barometer indicate that the peak of metamorphism (stage II) occurred at conditions of around 900 °C and 4 GPa. These results suggest that garnet peridotites in the Pohorje Mountains experienced UHPM during the Cretaceous orogeny. We propose that UHPM resulted from deep subduction of continental crust, which incorporated mantle peridotites from the upper plate, in an intracontinental subduction zone. Sinking of the overlying mantle and lower crustal wedge into the asthenosphere (slab extraction) caused the main stage of unroofing of the UHP rocks during the Upper Cretaceous. Final exhumation was achieved by Miocene extensional core complex formation.

Key words: Alps; garnet peridotite; Pohorje; slab extraction; ultrahigh-pressure metamorphism.

INTRODUCTION

Garnet-bearing peridotites occur within many collisional orogenic belts that underwent high-pressure (HP) and ultrahigh-pressure (UHP) metamorphism. These so-called 'orogenic' or 'Alpine-type' peridotites include several garnet-bearing rock types, such as lherzolites, harzburgites, wehrlites, dunites and pyroxenites, generally referred to as garnet peridotites. These rocks mostly occur not only within metamorphosed continental crust, but also within units of oceanic affinity (e.g. Brueckner & Medaris, 2000 and references therein). Garnet peridotites are commonly associated with eclogites in UHP metamorphic terranes (Liou *et al.*, 1998; Carswell & Compagnoni, 2003; Chopin, 2003). Although volumetrically minor, these UHP metamorphic rocks can provide important information on orogenic processes in deep orogenic root zones and the upper mantle (e.g. Zhang *et al.*, 1994; Dobrzhinetskaya *et al.*, 1996; Van Roermund & Drury, 1998). Most peridotites are incorporated into the subducted continental crust from the overlying mantle wedge (Brueckner & Medaris, 2000; Medaris, 2000). Lower-pressure protoliths (spinel-bearing peridotites) may be carried to deeper levels within the host continental slab and develop garnet-bearing assemblages at HP and UHP conditions of metamorphism. As an alternative, crustal peridotites (e.g. ophiolite components or ultramafic differentiates of mafic intrusions) may be subducted together with other crustal rocks and transformed to garnet peridotite.

This paper presents the evidence for UHP metamorphism of garnet-bearing ultramafic rocks in the Austroalpine units of the Eastern Alps, exposed in the Pohorje Mountains of Slovenia. In this area, Janák *et al.* (2004) have recently documented UHP metamorphism in kyanite eclogites. The evidence for UHP metamorphism in these eclogites comes both from geothermobarometry, which yields *P–T* conditions of 3.0–3.1 GPa and 760–825 °C, and microtextures such as: (i) polycrystalline quartz inclusions in garnet, omphacite and kyanite surrounded by radial fractures, and (ii) quartz rods in omphacite, which indicates an exsolution from a pre-existing supersilicic clinopyroxene that contained a Ca-Eskola component. In contrast, Sassi *et al.* (2004), using samples from almost the same area, determined lower maximum pressures of 1.8–2.5 GPa and questioned the UHP metamorphism. The eclogites are closely associated with serpentinized metaultrabasites in which few garnet peridotite remnants are preserved. Early estimates of the *P–T* conditions experienced by the Pohorje garnet peridotites were in the range of 750–1050 °C and 2.4–3.6 GPa (Hinterlechner-Ravnik *et al.*, 1991; Visona *et al.*, 1991).

Described here are the mineralogical and petrologic features of garnet peridotites, which constrain their metamorphic evolution to an initial, most probably spinel lherzolite stage, a UHP metamorphism stage and subsequent retrogression during exhumation.

This history is supported by thermobarometric results obtained from the various mineral assemblages. On the basis of petrochemical data, the pre-metamorphic origin of the peridotites is discussed. However, resolving the initial setting of their protolith is beyond the scope of this paper.

The results are additional evidence for UHP metamorphism in the Eastern Alps. We suggest that the possible mantle fragments (garnet peridotite) and the crustal rocks (eclogite) in the Pohorje Mountains experienced a common UHP metamorphism stage. We propose that this resulted from deep subduction of a continental slab, which incorporated the peridotites. It is shown that UHP rocks in the Pohorje Mountains were probably buried in an intracontinental subduction zone. Finally, the exhumation mechanism is discussed.

GEOLOGICAL BACKGROUND

Garnet peridotite bodies in the Alps are known from Alpe Arami, Monte Duria and Cima di Gagnone in the Adula-Cima Lunga unit (Ernst, 1978; Nimis & Trommsdorff, 2001; Paquin & Altherr, 2001), and from the Nonsberg area in the Ulten zone (Obata & Morten, 1987; Nimis & Morten, 2000). Those from the Adula-Cima Lunga unit are of Tertiary age (Becker, 1993; Gebauer, 1996), whereas those from Nonsberg are of Variscan age (Tumiati *et al.*, 2003). Metamorphic processes related to the Cretaceous, the so-called 'Eo-Alpine' events, in the Alps have been recognized mainly in the Austroalpine units (e.g. Thöni & Jagoutz, 1992; Hoinkes *et al.*, 1999; Schmid *et al.*, 2004; Schuster *et al.*, 2004). In the Eastern Alps, the metamorphic grade of Cretaceous metamorphism reached UHP facies in the south-easternmost parts, in the Pohorje Mountains of Slovenia, belonging to the Lower Central Austroalpine unit (Janák *et al.*, 2004; Oberhänsli *et al.*, 2004). Regional south-eastward increase of peak pressures in this unit indicates a south to eastward dip of the subduction zone.

The HP metamorphism is commonly interpreted to be related to the collision between the Austroalpine and another continental fragment or an island arc after the closure of the Meliata-Hallstatt Ocean (e.g. Thöni & Jagoutz, 1992; Froitzheim *et al.*, 1996; Stampfli *et al.*, 1998). Janák *et al.* (2004) suggested that subduction was intracontinental; NW parts of the Austroalpine (Lower Central Austroalpine) were subducted under SE parts (Upper Central Austroalpine). The subduction zone formed in the Early Cretaceous, in the NW foreland of the Meliata suture after Late Jurassic closure of the Meliata Ocean and resulting collision (Janák *et al.*, 2004). The intracontinental subduction zone was localized in a Permian-age continental rift, as evidenced by remnants of Permian rifting-related HT/LP amphibolite-facies metamorphism in the same units of the Lower Central Austroalpine that were later affected by Alpine HP/UHP metamorphism (Schuster *et al.*, 2004).

The Pohorje Mountains are built up of three Eoalpine Cretaceous nappes (Mioč & Žnidarčič, 1977; Fodor *et al.*, 2003) that belong to the pre-Neogene, metamorphic sequences within the Austroalpine units of the Eastern Alps (Fig. 1). The lowest nappe, which represents the Lower Central Austroalpine (Janák *et al.*, 2004), consists of medium to high-grade metamorphic rocks, predominantly micaschists, gneisses and amphibolites with marble and quartzite lenses. We propose that this nappe be termed the 'Pohorje nappe'. The nappe also contains several eclogite lenses and a body of ultramafic rocks (Fig. 2). It is overlain by a nappe composed of weakly metamorphosed Palaeozoic rocks, mainly low-grade metamorphic slates and phyllites. The uppermost nappe is built up of Permo-Triassic clastic sediments, mainly sandstones and conglomerates. The two latter nappes represent the Upper Central Austroalpine. This nappe stack is overlain by Early Miocene sediments, which belong to syn-rift basin fill of the Pannonian Basin (Fodor *et al.*, 2003). The magmatic intrusion in the central part of Pohorje, which was emplaced along the Periadriatic fault system during Oligocene to Miocene (Altherr *et al.*, 1995), is of mainly granodioritic to tonalitic composition. The Pohorje nappe is folded into an ESE–WNW-striking antiform, the core of which is occupied by the intrusion. Therefore, neither the original basal contact of the Pohorje nappe nor any deeper tectonic units are exposed in the Pohorje area.

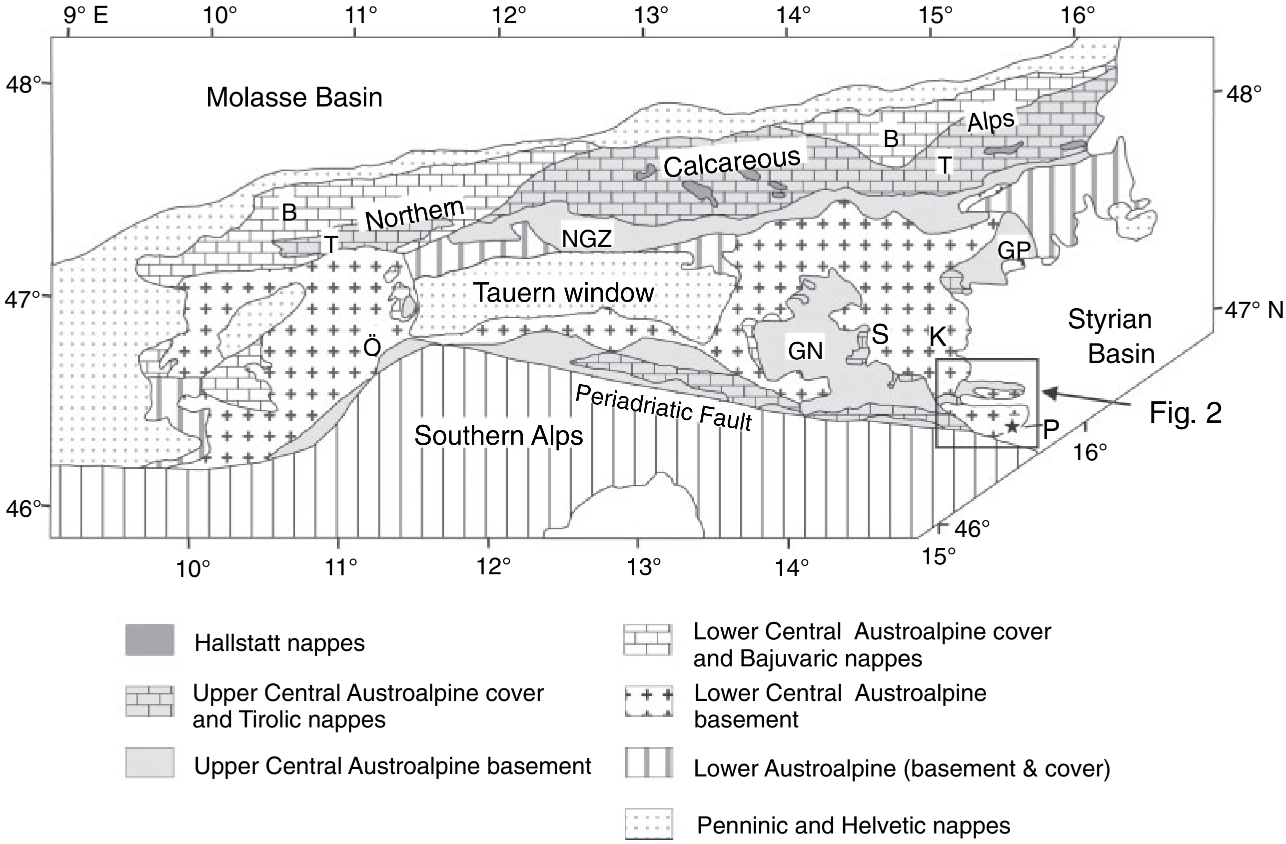

Fig. 1. Tectonic map of the Eastern Alps; B, Bajuvaric; GN, Gurktal nappe; GP, Graz Paleozoic; K, Koralpe; NGZ, Northern Grauwacke zone; Ö, Southern Ötztal nappe; P, Pohorje; S, Saualpe; T, Tirolic. Modified after Neubauer & Höck (2000) and Schmid *et al.* (2004).

Metaultrabasites occur in the south-easternmost part of Pohorje Mountains near Slovenska Bistrica (Fig. 2), where they form a body of *c.* 5 × 1 km size, which is termed the 'Slovenska Bistrica ultramafic complex' (SBUC). However, garnet peridotites also occur away from this body, as is the case for locality 119 (Fig. 2). The main protoliths of the SBUC are harzburgites and dunites (cf. Hinterlechner-Ravnik, 1987; Hinterlechner-Ravnik *et al.*, 1991). Because of extensive serpentinization, only a few less altered garnet peridotites, garnet pyroxenites and coronitic metatroctolites are preserved (Hinterlechner-Ravnik, 1987; Hinterlechner-Ravnik *et al.*, 1991). The ultrabasites include numerous lenses, boudins and bands of eclogites. The country rocks of the SBUC are amphibolites, orthogneisses, paragneisses and micaschists. These rocks form a strongly foliated matrix around elongated lenses and boudins of eclogite and ultrabasite, including the SBUC. The foliation and orientation of the lenses are parallel to the upper boundary of the Pohorje nappe. The foliation formed during exhumation, as can be seen from the amphibolitization of eclogite in those zones where it shows the foliation, that is, mostly along the margins of eclogite boudins.

The timing of HP and UHP metamorphism in the Pohorje nappe is Cretaceous, as shown by a garnet Sm-Nd age (93–87 Ma) obtained from the gneisses and micaschists (Thöni, 2002), and by *c.* 90 Ma garnet Sm-Nd and zircon U-Pb ages of eclogites (Miller *et al.*, 2005). This age is similar to that of Koralpe and Saualpe eclogite facies metamorphism (Thöni & Jagoutz, 1992; Thöni & Miller, 1996; Miller & Thöni, 1997; Thöni, 2002). Tertiary K-Ar mica ages (19–13 Ma) as well as apatite and zircon fission track ages (19–10 Ma) were obtained from the country rocks of eclogites and metaultrabasites in the Pohorje nappe (Fodor *et al.*, 2002). This suggests that the peak of metamorphism was attained during the Cretaceous, and final cooling occurred in the Early to Middle Miocene. Upper Cretaceous (75 to 70 Ma) cooling ages were determined in the Koralpe area, the north-westward extension of the Pohorje nappe (Fig. 2; Schuster *et al.*, 2004), indicating that the Koralpe rocks were exhumed during the Upper Cretaceous. The main exhumation of the Pohorje nappe, from UHP depth to crustal depth, most probably occurred during the Upper Cretaceous as well, and only the late stage of exhumation to the surface was achieved in the Miocene, by east- to

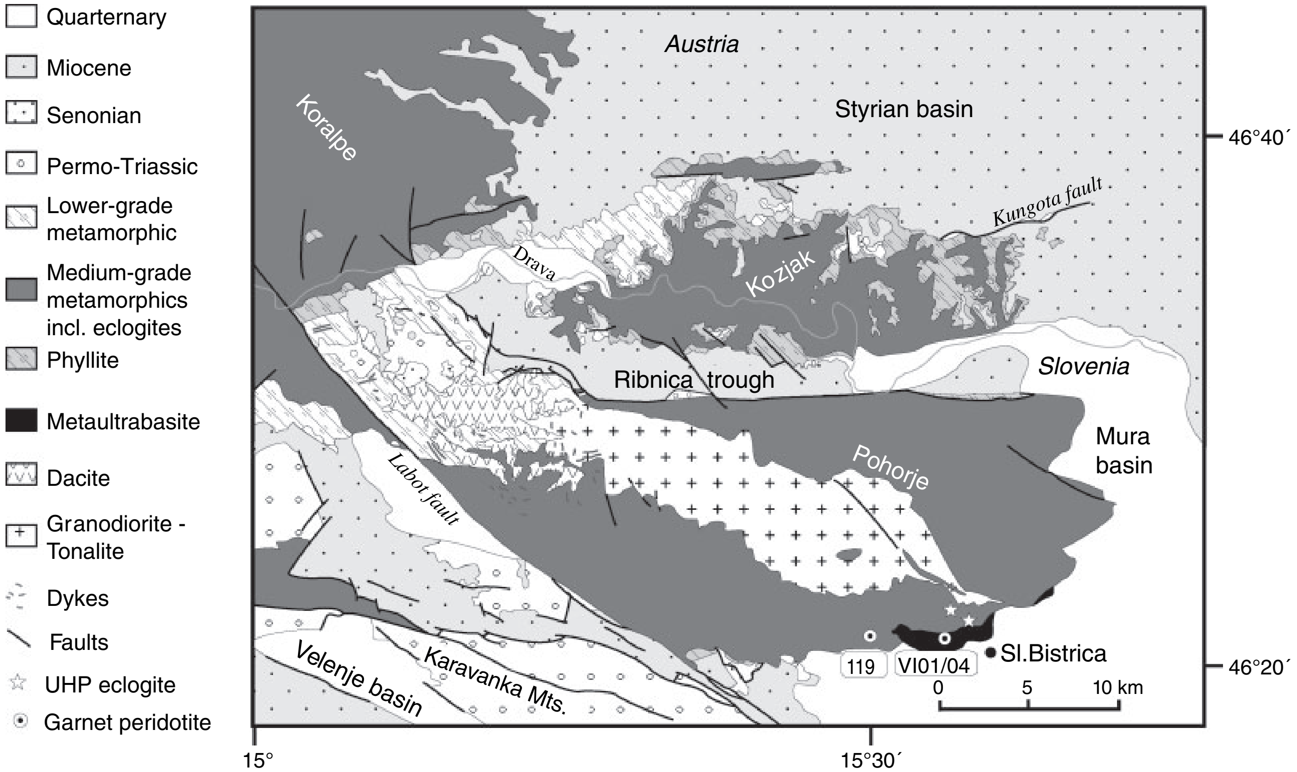

Fig. 2. Simplified geological map of Pohorje and adjacent areas (modified from Mioč & Žnidarčič (1977) showing locations of the investigated garnet peridotites.

north-east-directed low-angle extensional shearing leading to the core-complex structure of the Pohorje Mountains (Fodor *et al.*, 2003). The Miocene shearing event reactivated and overprinted the nappe boundaries in the Pohorje area. Therefore, direct structural evidence for the kinematics of Cretaceous exhumation has not yet been found.

PETROGRAPHY AND MINERAL CHEMISTRY

Disregarding deeply serpentinized rocks, several samples of relatively well-preserved garnet peridotites from two localities (Fig. 2) were investigated. One locality (VI01/04) is within the SBUC near Visole and one (119) is farther west, near Modrič. The garnet-bearing peridotites occur as tens of centimetre to metre sized blocks and lenses within the extensively serpentinized ultrabasites. Garnet peridotites exhibit rather massive and relatively homogeneous textures without any distinct compositional layering on the hand-specimen and thin-section scale.

These rocks consist of garnet, olivine, orthopyroxene, clinopyroxene and brown spinel, which are variably replaced by amphibole, green spinel, serpentine, talc and chlorite. They show higher modal amounts of garnet and clinopyroxene relative to olivine, particularly in the samples from Modrič (119). This suggests a pyroxenite (garnet-olivine websterite) origin of these metaultrabasites. However, because of retrogression, the abundance of primary minerals is largely obscured.

Microstructures along with variations in mineral chemistry suggest that the metaultramafic rocks have experienced a complex metamorphic history. Table 1 shows representative analyses of the main constituent minerals determined using a CAMECA SX-100 electron microprobe at Dionýz Štúr Institute of Geology in Bratislava. Analytical conditions were 15 kV accelerating voltage and 20 nA beam current, with a peak counting time of 20 s and a beam diameter of 2–10 μm. Raw counts were corrected using a PAP routine. Mineral abbreviations are according to Kretz (1983). At least four stages of recrystallization have been identified in the garnet peridotite.

Stage I

This stage is defined by assemblage of olivine + orthopyroxene + clinopyroxene + Cr-spinel. Chromian spinel occurs in the matrix and as inclusions in garnet (Fig. 3a). This spinel is mostly opaque at the rims and brown in the core. The opaque spinel has a higher chromium number [$Cr^* = 100 \times Cr/(Cr + Al) =$ 47–52] than the brown spinel ($Cr^* = 22$–43). Inclusions of clinopyroxene in garnet contain up to 4.9 wt% Al_2O_3, whereas orthopyroxene inclusions have 1.7–2 wt% Al_2O_3.

Table 1. Representative electron microprobe analyses of minerals.

Sample:	VI01/04	VI01/04	VI01/04	VI01/04	VI01/04	VI01/04	VI01/04	VI01/04	VI01/04	VI01/04	VI01/04
Mineral:	Ol	Grt	Cpx	Cpx	Opx	Opx	Opx	Spl	Spl	Amp	Amp
Stage:	II	II	I	II–III	I	II	III	I–II	III	III	IV
SiO_2	40.45	42.18	52.95	54.91	57.20	57.56	56.79	0.01	0.54	44.70	58.03
TiO_2	0.00	0.00	0.00	0.02	0.00	0.01	0.00	0.12	0.05	0.09	0.01
Al_2O_3	0.01	23.12	4.87	0.96	1.71	0.82	1.54	24.41	65.65	15.24	1.22
Cr_2O_3	0.00	0.52	0.16	0.17	0.00	0.02	0.01	38.71	0.81	0.81	0.10
FeO	11.63	10.66	3.36	1.88	6.86	7.55	7.84	24.97	12.22	3.45	1.93
MnO	0.15	0.35	0.09	0.05	0.09	0.21	0.26	0.37	0.08	0.05	0.05
NiO	0.33										
MgO	48.35	18.05	17.65	17.63	34.06	34.00	33.97	10.00	19.97	17.71	23.21
CaO	0.01	5.67	21.32	24.63	0.30	0.10	0.14	0.02	0.28	13.03	13.45
Na_2O	0.00	0.00	0.29	0.32	0.00	0.00	0.01	0.00	0.00	2.26	0.07
K_2O	0.00	0.00	0.01	0.01	0.01	0.00	0.00	0.00	0.00	0.07	0.01
Total	100.93	100.55	100.70	100.58	100.23	100.27	100.56	98.61	99.60	97.41	98.08
Si	0.99	3.01	1.90	1.98	1.97	1.99	1.96	0.00	0.01	6.28	7.89
Ti	0.00	0.00	0.00	0.00	0.00	0.00	0.00	0.00	0.00	0.01	0.00
Al	0.00	1.94	0.21	0.04	0.07	0.03	0.06	0.90	1.95	2.52	0.20
Cr	0.00	0.03	0.01	0.01	0.00	0.00	0.00	0.96	0.02	0.09	0.01
Fe^{2+}	0.24	0.64	0.10	0.06	0.20	0.22	0.23	0.65	0.26	0.40	0.22
Mn	0.00	0.02	0.00	0.00	0.00	0.01	0.01	0.01	0.00	0.01	0.01
Ni	0.01										
Mg	1.77	1.92	0.94	0.95	1.75	1.75	1.74	0.47	0.75	3.71	4.70
Ca	0.00	0.43	0.82	0.95	0.01	0.00	0.01	0.00	0.01	1.96	1.96
Na	0.00	0.00	0.02	0.02	0.00	0.00	0.00	0.00	0.00	0.62	0.02
K	0.00	0.00	0.00	0.00	0.00	0.00	0.00	0.00	0.00	0.01	0.00
Total	3.01	8.00	4.00	4.00	3.99	4.00	4.00	3.00	2.99	15.60	15.01
X_{Mg}	0.88	0.75	0.90	0.94	0.90	0.89	0.89	0.42	0.74	0.90	0.96
Cr*								0.52	0.01		
Sample:	119-5	119-5	119-5	119-5	119-5	119-5	119-5	119-5	119-5	119-5	119-5
Mineral:	Ol	Grt	Grt	Cpx	Opx	Opx	Opx	Spl	Spl	Amp	Amp
Stage:	II	exs[a]	II	I–II	exs	II	III	I–II	III	III	IV
SiO_2	40.69	42.19	41.32	55.31	58.30	58.25	56.52	0.00	0.03	45.44	55.18
TiO_2	0.00	0.02	0.00	0.10	0.05	0.03	0.00	0.27	0.01	0.50	0.22
Al_2O_3	0.03	22.88	23.39	1.30	0.84	0.73	1.64	24.29	68.21	13.28	3.72
Cr_2O_3	0.01	1.28	0.03	0.67	0.20	0.09	0.00	37.45	0.16	1.45	0.62
FeO	10.69	12.31	10.04	1.88	7.00	6.45	6.88	25.58	8.33	3.75	2.11
MnO	0.10	0.35	0.24	0.01	0.08	0.08	0.04	0.40	0.02	0.01	0.04
NiO	0.32										
MgO	49.90	17.00	18.36	17.29	35.20	35.70	34.54	9.68	22.43	19.33	22.63
CaO	0.02	5.91	5.90	23.66	0.29	0.17	0.19	0.01	0.07	11.86	13.21
Na_2O	0.00	0.00	0.00	0.63	0.00	0.00	0.00	0.00	0.00	2.82	0.72
K_2O	0.00	0.00	0.00	0.01	0.00	0.00	0.00	0.00	0.00	0.02	0.02
Total	101.76	101.94	99.28	100.86	101.96	101.50	99.81	97.68	99.26	98.70	98.61
Si	0.99	3.00	2.98	1.99	1.97	1.97	1.95	0.00	0.00	6.33	7.51
Ti	0.00	0.00	0.00	0.00	0.00	0.00	0.00	0.01	0.00	0.05	0.02
Al	0.00	1.92	1.99	0.06	0.03	0.03	0.07	0.91	1.99	2.18	0.60
Cr	0.00	0.07	0.00	0.02	0.01	0.00	0.00	0.94	0.00	0.16	0.07
Fe^{2+}	0.22	0.73	0.61	0.06	0.20	0.18	0.20	0.68	0.17	0.44	0.24
Mn	0.00	0.02	0.02	0.00	0.00	0.00	0.00	0.01	0.00	0.00	0.01
Ni	0.01										
Mg	1.80	1.80	1.97	0.93	1.78	1.80	1.78	0.46	0.83	4.01	4.59
Ca	0.00	0.45	0.46	0.91	0.01	0.01	0.01	0.00	0.00	1.77	1.93
Na	0.00	0.00	0.00	0.04	0.00	0.00	0.00	0.00	0.00	0.76	0.19
K	0.00	0.00	0.00	0.00	0.00	0.00	0.00	0.00	0.00	0.00	0.00
Total	3.02	7.99	8.02	4.00	4.00	3.99	4.00	3.00	3.00	15.71	15.16
X_{Mg}	0.89	0.71	0.77	0.94	0.90	0.91	0.90	0.40	0.83	0.90	0.95
Cr*								0.51	0.00		

[a]Exsolved from clinopyroxene.

Stage II

Here, the metamorphic stage is defined by the matrix assemblage garnet + clinopyroxene + orthopyroxene + olivine + Cr-spinel. Garnet occurs as coronas around Cr-spinel, exsolutions from clinopyroxene, and large porphyroblasts in the matrix. These are inhomogeneous, showing an irregular distribution of composition. The abundances of Mg, Fe and Ca in garnet are significantly variable, with *mg*-number [$100 \times Mg/(Mg + Fe)$] ranging from 66 to 77. Small, exsolved garnet has lower Mg and higher Cr contents than large matrix garnet. Clinopyroxene is diopsidic with low Na_2O and Cr_2O_3 contents. Primary, coarse-grained clinopyroxene contains exsolution rods of garnet, low-Al orthopyroxene, pargasitic amphibole, Cr-spinel and ilmenite (Fig. 3b). Matrix orthopyroxene grains (Fig. 3c) are inhomogeneous with respect to

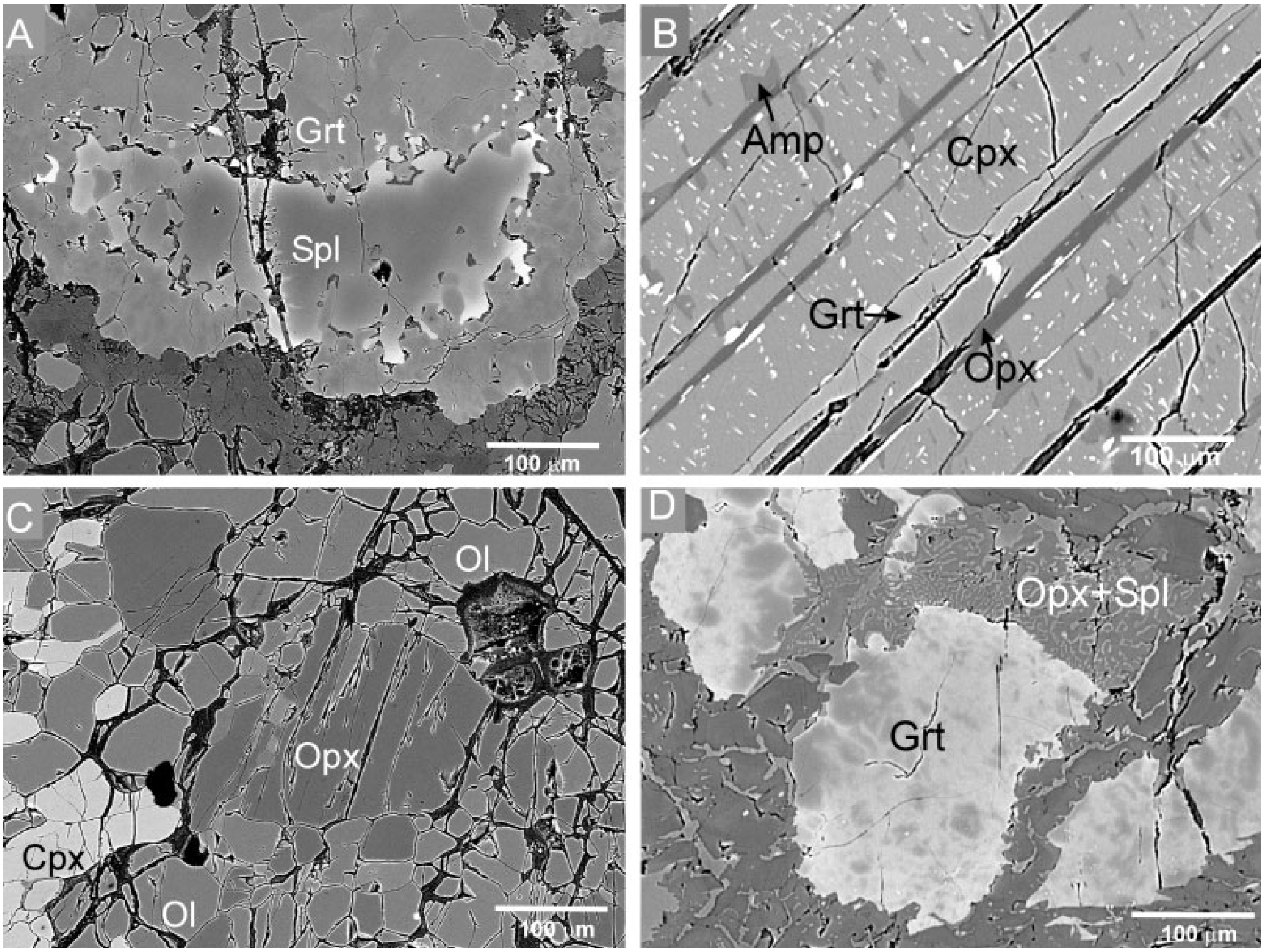

Fig. 3. Photomicrographs (backscattered electron images) of garnet peridotites. (a) Spinel (Spl) inclusion in garnet porphyroblast (sample 119-5). (b) Clinopyroxene (Cpx) with exsolutions of garnet (Grt), orthopyroxene (Opx) and pargasitic amphibole (Amp). Bright patches are Cr-spinel and ilmenite (sample 119-5). (c) Stage II assemblage of olivine (Ol), orthopyroxene (Opx) and clinopyroxene (Cpx) in the matrix (sample 119-5). (d) Symplectite of orthopyroxene (Opx) and spinel (Spl) replacing garnet (Grt). Note the darker (Mg-rich) and brighter (Fe-rich) compositions in garnet (sample VI01/04).

Al, Fe and Mg. Exsolved orthopyroxene has lower Al than inclusions in garnet, but the lowest contents of Al_2O_3 (0.73 wt%) are found in larger, recrystallized orthopyroxene grains. The distribution of Al with respect to cores and rims is rather irregular. Olivine grains are nearly homogeneous. There are, however, some differences in the abundance of Mg and Fe (*mg*-number = 88–91) between individual olivine grains. The chemical homogeneity of olivine may be explained by the fact that Fe-Mg diffusion in olivine is about two orders of magnitude faster than that in pyroxene and garnet (Brenker & Brey, 1997).

Stage III

In this stage decompression after peak pressure conditions is manifested by the formation of kelyphitic rims of high-Al orthopyroxene (2–3 wt% Al_2O_3), aluminous spinel (Cr* = 0.6–0.9), diopside and pargasitic amphibole replacing garnet (Fig. 3d). As a result of retrogression, garnet shows a decrease in Mg and increase in Fe.

Stage IV

Here, retrogression under lowest *P–T* conditions is represented by formation of tremolitic amphibole, gedrite, chlorite, serpentine and talc, which have partly replaced olivine and pyroxene.

GEOCHEMISTRY OF PERIDOTITES

Major elements were determined at ACME Analytical Laboratories (Vancouver, Canada) by ICP-ES analysis using a $LiBO_2$ fusion. Loss on ignition (LOI) was determined after ignition of 1 g powder at 1000 °C. Trace elements were determined by ICP-MS in the Dept. of Geology at Göteborg University, Sweden,

Table 2. Major and trace-element concentrations of Pohorje peridotites.

	VI01/04	119-4	119-5	119-6
wt%				
SiO_2	38.54	41.83	43.56	42.54
Al_2O_3	7.65	11.82	9.92	12.43
Cr_2O_3	0.24	0.14	0.29	0.23
$Fe_2O_3^T$	8.24	9.85	9.12	10.81
MnO	0.10	0.16	0.14	0.17
MgO	30.53	25.92	26.61	24.57
CaO	2.19	6.62	7.57	6.56
Na_2O	0.23	0.95	0.61	0.96
LOI	12.30	2.65	1.71	1.44
SUM	100.02	99.94	99.53	99.71
ppm				
Li	26	5.6	2.4	6.0
P	17	73	20	47
K	208	144	98	712
Sc	5	9	17	12
Ti	164	1105	480	640
V	21	63	59	73
Co	96	100	81	103
Ni	1595	1095	1115	1035
Cu	23	40	58	19
Zn	41	56	30	63
Sr	17	58	36	41
Y	0.50	4.3	2.7	3.0
Zr	0.57	7.1	1.9	6.4
Ba	45	2.0	5.5	15
ppb				
As	574	227	840	552
Rb	1075	454	317	1440
Nb	160	138	76	120
Sn	225	211	526	192
Sb	46	24	60	46
Cs	587	107	61	215
La	203	302	657	271
Ce	519	1175	308	721
Pr	69	226	157	171
Nd	346	1460	750	1183
Sm	79	502	236	487
Eu	68	209	138	227
Gd	102	683	365	665
Tb	15	124	65	104
Dy	104	840	449	638
Ho	19	177	98	125
Er	59	518	295	331
Tm	10	72	40	47
Yb	70	478	264	296
Lu	12	76	42	47
Pb	532	344	332	994
Th	30	5	3	4
U	6	2	3	2

Major elements by ICP-ES; trace elements by ICP-MS; LOI, loss on ignition; all Fe reported as Fe_2O_3.

following a HF-HNO_3 digestion procedure. The accuracy of the analysis was monitored on international rock standards UB-N (serpentinite), NIM-P (pyroxenites) and NIM-D (dunite); our values are generally within 10% of the recommended values. Precision of duplicate analyses is better than 5% for all elements except Nb, Sn, Sb, Th, and U (10–30%), partially because of the low levels of these elements. The analyses are listed in Table 2.

In accordance with the high modal amounts of garnet and clinopyroxene, the rocks are rich in Al_2O_3 (7.7–12.4 wt%) and CaO (2.2–7.6 wt%) relative to primitive mantle (4.45 and 3.35 wt% respectively; McDonough & Sun, 1995), whereas MgO contents are relatively low (25–30 wt%). Compared with primitive mantle, the '119' samples show a depletion in incompatible elements (Fig. 4), with the exception of alkaline and earth-alkaline metals and Pb, and the pattern is quite similar to that of depleted MORB mantle (DMM; Workman & Hart, 2005). Moreover, a slight negative Zr anomaly is observed, but other HFSE are not depleted. The VI01/04 sample is much more depleted than the '119' samples, but shows similar positive anomalies in (earth) alkalis, Pb and Zr. REE patterns (Fig. 5) are characterized by relatively straight patterns, showing slight LREE depletion for two of the '119' samples and LREE enrichment for the VI01/04 sample, which is considerably more HREE depleted than the other samples. Most samples show positive Eu anomalies, and one sample, 119-5, shows a peculiar strongly negative Ce-anomaly. The significance of these patterns will be discussed later.

GEOTHERMOBAROMETRY

Metamorphic *P–T* conditions have been calculated from a combination of (i) garnet-olivine (O'Neill & Wood, 1979) and garnet-orthopyroxene (Harley, 1984) Fe-Mg exchange thermometers, and (ii) the Al-in-orthopyroxene barometer (Brey & Köhler, 1990). Fe-Mg exchange thermometry between garnet, olivine and orthopyroxene is compromised by uncertainties in the Fe^{3+} content in these phases. All Fe has therefore been treated as Fe^{2+} in the calculations.

Utilizing the compositions of garnet and orthopyroxene exsolutions in primary clinopyroxene from sample 119-5 (Table 1), application of Fe-Mg partitioning between coexisting garnet and orthopyroxene as thermometer together with the Al-in orthopyroxene barometer yields *P–T* values of 730 °C and 2.6 GPa. These may correspond to initial metamorphic conditions of garnet formation.

Porphyroblastic garnet with the highest pyrope content and orthopyroxene with the lowest Al content together with relatively homogeneous olivine have been chosen to calculate peak *P–T* conditions, as it is generally recommended (e.g. Brey & Köhler, 1990; Brenker & Brey, 1997; Krogh Ravna & Paquin, 2003). The results obtained from the *P–T* intersections calculated from selected compositions of garnet, olivine and orthopyroxene (stage II in Table 1) are presented in Table 3 and Fig. 6.

The equilibrium *P–T* conditions for sample 119-5 cluster in a narrow range, close to values of 900 °C and 4 GPa. There is a very good consistency between the garnet-olivine and garnet-orthopyroxene thermometers for this sample. The *P-T* conditions for sample VI01/04, obtained from the garnet-olivine thermometer and the Al-in-orthopyroxene barometer, are 887 °C and 3.4 GPa, whereas the intersection between the garnet-orthopyroxene thermometer and the Al-in-orthopyroxene barometer yields 962 °C and 3.85 GPa. This discrepancy may result from partial

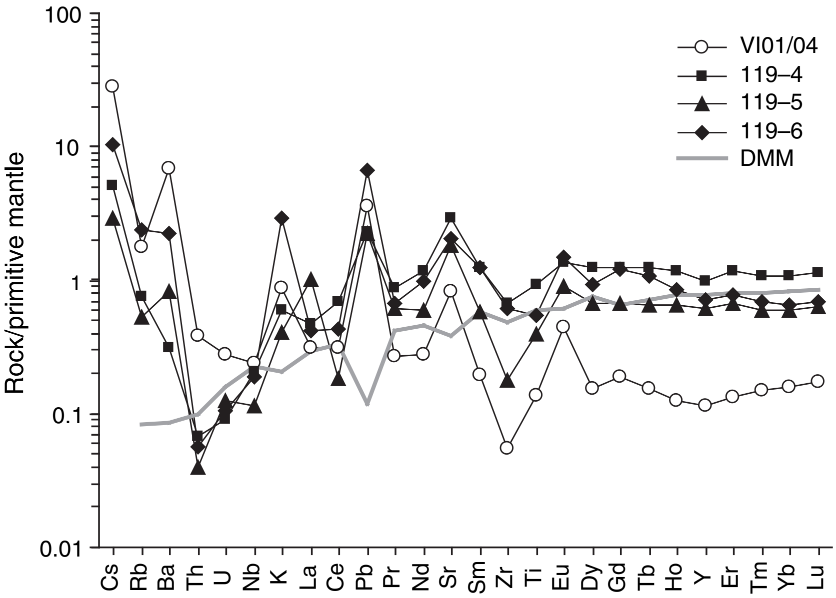

Fig. 4. Whole-rock trace-element compositions of Pohorje peridotites relative to primitive mantle (McDonough & Sun, 1995). The grey line indicates the composition of depleted MORB mantle (DMM) according to Workman & Hart (2005).

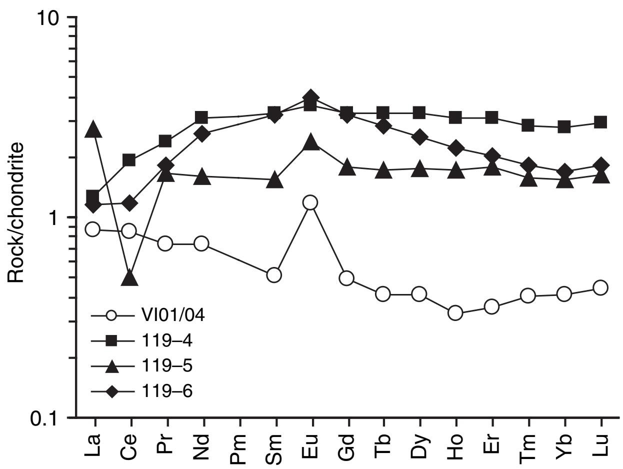

Fig. 5. Whole-rock REE compositions of Pohorje peridotites relative to CI chondrite (McDonough & Sun, 1995). Note the conspicuous positive Eu anomalies and the negative Ce anomaly of one of the samples.

disequilibrium between garnet, olivine and orthopyroxene during post-peak decompression.

DISCUSSION

P–T path

The microtextural and thermobarometric evidence described above indicates that garnet-bearing peridotites in the Pohorje Mountains have experienced a complex history. A metamorphic *P–T* path for these peridotites (Fig. 7) can be deduced from the observed mineral assemblages and estimated *P–T* conditions. The occurrence of spinel as inclusions in garnet indicates that garnet peridotites evolved from spinel-bearing protoliths (stage I), which could therefore represent pieces of intermediate to shallow-level lithospheric mantle.

Table 3. *P–T* intersection values for the peak metamorphic stage of garnet peridotites.

	Grt-Ol (OW 79) + Al-in-Opx (BK 90)		Grt-Opx Fe-Mg (H 84) + Al-in-Opx (BK 90)	
Sample	*P* (GPa)	*T* (°C)	*P* (GPa)	*T* (°C)
VI01/04	3.36	887	3.85	962
119-5	4.03	902	4.02	900

Formation of garnet exsolutions from clinopyroxene could have started at *P–T* conditions of about 700–750 °C and 2.5 GPa (Fig. 7), as deduced from geothermobarometry. The exsolution process may correspond to the incorporation of peridotite into a subducting crust from the overlying mantle wedge. Similar exsolutions have been observed in other HP and UHP ultramafic rocks, e.g. garnet peridotite and pyroxenite from Nonsberg area, Eastern Alps (Godard *et al.*, 1996), garnet clinopyroxenite from Sulu, eastern China (Zhang & Liou, 2003) and garnet websterite from Bardane, western Norway (Carswell & Van Roermund, 2005).

The peak of metamorphism is defined by the matrix assemblage garnet + olivine + orthopyroxene + clinopyroxene + Cr-spinel. Based on microtextural observations described above, we assume that garnet was formed from primary, Al-bearing phases such as spinel, clinopyroxene and orthopyroxene according to the reaction:

$$\mathrm{Spl + Cpx + Opx = Grt + Ol} \qquad (1)$$

Based on the increased chromium content in the rims, it is assumed that Cr-rich spinel ($Cr^* = c.\ 50$)

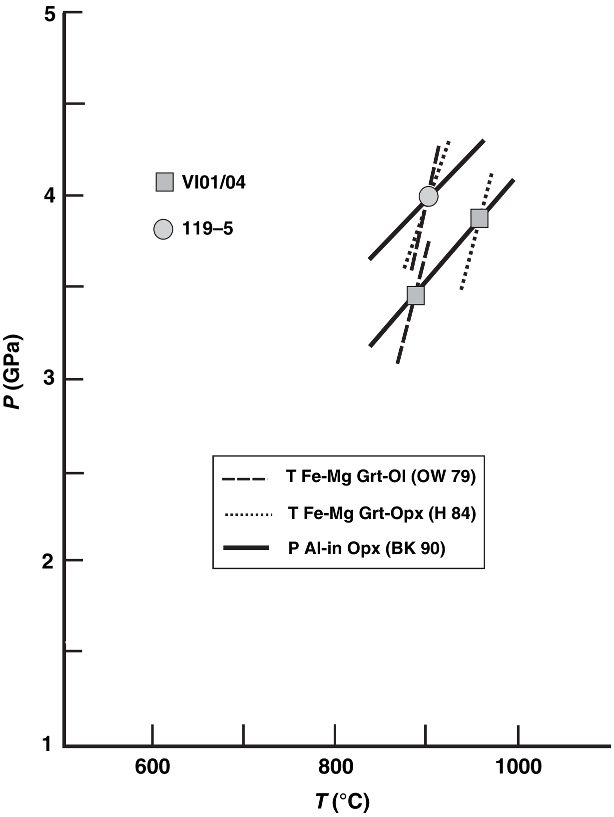

Fig. 6. Results from geothermobarometry for garnet peridotites (samples VI01/04 and 119-5) using the garnet-olivine (O'Neill & Wood, 1979) and garnet-orthopyroxene (Harley, 1984) Fe-Mg exchange thermometers and Al-in orthopyroxene (Brey & Köhler, 1990) geobarometer.

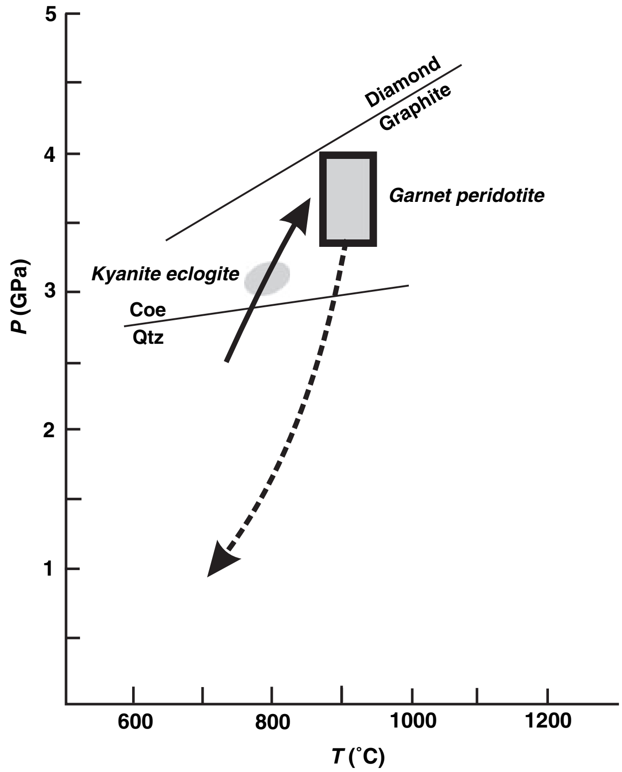

Fig. 7. Metamorphic pressure–temperature path of the garnet peridotites from the Pohorje Mountains Peak metamorphic conditions of the associated kyanite eclogites after Janák *et al.* (2004). The quartz–coesite and graphite-diamond curves are calculated from the thermodynamic data of Holland & Powell (1998).

remained stable at peak metamorphic conditions since chromium expands the spinel-garnet transition towards higher pressures (Webb & Wood, 1986; Klemme, 2004). *P–T* conditions of the peak metamorphic stage calculated from geothermobarometry are 890–960 °C and 3.4–4 GPa. The associated kyanite eclogites reached 760–825 °C and 3–3.1 GPa (Janák *et al.*, 2004). Both the garnet peridotites and eclogites show maximum *P–T* conditions within the stability field of coesite (Fig. 7). The data obtained from garnet peridotites thus clearly confirm the existence of UHP metamorphism in the Pohorje area.

Microtextural observations suggest that, after having reached their metamorphic peak, the garnet peridotites were exhumed to mid-crustal levels. During this stage (stage III), garnet decomposed to alumina-rich spinel, orthopyroxene and clinopyroxene symplectites. The development of the kelyphitic assemblage may have resulted from the decompression reaction:

$$\text{Grt} + \text{Ol} = \text{Opx} + \text{Cpx} + \text{Spl} \quad (2)$$

As mineral compositions of the kelyphitic assemblage vary, implying disequilibrium between the reactants and products, we were unable to evaluate the *P–T* conditions of stage III. Formation of pargasitic amphibole from garnet and clinopyroxene may have occurred according to the reaction:

$$\text{2Di-Cpx} + \text{Grt} + H_2O = \text{Prg-Amp} \quad (3)$$

It is assumed that decompression occurred at still high temperatures, as has been deduced also from the presence of sapphirine + spinel + corundum symplectites after kyanite in the associated eclogites (Janák *et al.*, 2004).

In the last stage (stage IV), pargasitic amphibole was partly replaced by tremolite, pyroxene by serpentine and chlorite, and olivine by serpentine and minor talc. It is assumed that during this stage, pressure and temperature further decreased, and increased activity of H_2O caused retrogression under low *P–T* conditions.

Petrogenesis of the Pohorje peridotites

The major element composition of the peridotites shows that these rocks cannot be residual mantle peridotites, but are likely to have undergone metasomatism by transient melts and/or fluids, as many fluid-mobile elements (Cs, Rb, Ba, K, Pb) show positive anomalies. Moreover, the rocks show positive anomalies of elements usually indicative of the presence of plagioclase (Sr, Eu, also CaO and Al_2O_3).

An origin as cumulates from mafic melts in the continental crust can be ruled out, as this cannot explain the generally depleted trace-element character of the rocks, despite their highly fertile major-element composition. Garnet websterites from the Beni Bousser Massif in Morocco (Pearson *et al.*, 1993) have compositions similar to the Pohorje peridotites, and are interpreted to be the result of crystal segregation along magma conduits in the garnet stability field. However, petrographic and mineralogical evidence indicates that the Pohorje peridotite protolith formed at low pressures outside the garnet-stability field. Becker (1996) reported rocks with similar major elements compositions from the Bohemian Massif in Austria and also suggested an origin by melt impregnation, but trace-element patterns are very different from those observed here. A few rocks interpreted as subducted crustal rocks that show signs of plagioclase accumulation have similar REE patterns as Pohorje peridotites, but are quite different in other respects, i.e. lower MgO, Cr, Ni, higher TiO_2 and very high Al_2O_3 and CaO contents (Becker, 1996).

We suggest two scenarios for the formation of the Pohorje garnet peridotites. The protoliths could have been depleted mantle rocks metasomatized by melts and/or fluids in the plagioclase stability field, in which plagioclase crystallized (cf. Müntener *et al.*, 2004). Alternatively, melts/fluids from plagioclase-bearing crustal rocks could have metasomatized the peridotite protolith in the spinel-peridotite field (cf. Pearson *et al.*, 1993) during subduction.

Tectonic scenario for UHP metamorphism and exhumation

Regardless of the origin of the Pohorje garnet peridotites, these rocks and associated kyanite eclogites experienced UHP metamorphism, most probably during the Cretaceous orogeny. It is proposed that UHP metamorphism resulted from deep subduction of a continental slab, which incorporated peridotites from an overlying mantle wedge (Fig. 8). The garnet-bearing assemblage developed under an increase in pressure, when the peridotites were carried to deeper levels within the host continental slab.

Subduction and the related HP/UHP metamorphism in the Austroalpine realm at *c.* 100 to 85 Ma (Thöni, 2002) were contemporaneous with the latest stage of oceanic accretion in the Penninic ocean (*c.* 93 Ma, Liati *et al.*, 2003). The subduction zone in which the Pohorje UHP rocks were buried dipped towards south or south-east (Fig. 8), as suggested by a generally south-eastward increase of metamorphic grade in the Austroalpine basement of the Eastern Alps (Oberhänsli *et al.*, 2004). The subduction zone was probably intracontinental. This is suggested by the facies, indicating deposition on continental crust of

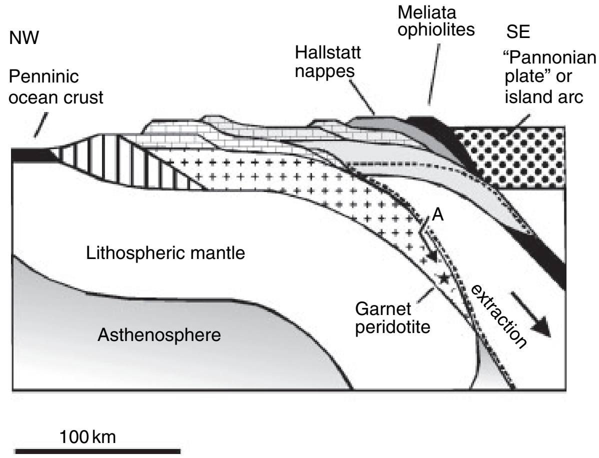

Fig. 8. Hypothetical cross-section of the Austroalpine orogen at *c.* 100 to 90 Ma. Patterns are the same as in Fig. 1. Pohorje garnet peridotites and kyanite eclogites are deeply buried in an intra-Austroalpine subduction zone. The peridotites were incorporated from the overlying mantle wedge and carried down to UHP depth (burial path 'A'). Exhumation was accommodated by later extraction of the Upper Central Austroalpine lower crustal and mantle wedge. The dashed line delineates the extracted wedge. It comprises lithospheric mantle (white) and lower crust (grey) of the Upper Central Austroalpine, as well as oceanic crust of the Meliata ocean (black).

Permian and Mesozoic sedimentary rocks in the Tirolic nappes of the Northern Calcareous Alps (Fig. 1), which represent the detached cover rocks of the Lower Central Austroalpine (Janák *et al.*, 2004).

The Pohorje nappe, like the Koralpe complex, is formed by typical Pre-Mesozoic continental basement. Basaltic melts with N-MORB geochemistry as described for Pohorje eclogites (Sassi *et al.*, 2004) are not restricted to the oceanic crust but may also be emplaced as dykes, sills or other intrusions within the continental crust during rifting (e.g. Desmurs *et al.*, 2002). The Lower Central Austroalpine, including the Pohorje nappe, formed the footwall, as it was subducted under the Upper Central Austroalpine representing the hanging wall (Fig. 8). Consequently, Cretaceous HP metamorphism is restricted to the Lower Central Austroalpine. The intracontinental subduction zone formed during the Cretaceous after the collisional closure of the Meliata Ocean, which occurred to the SE and is marked by ophiolites of the Meliata suture. The Meliata Ocean had closed either by continent–continent (Plašienka, 1995) or arc–continent collision (Stampfli *et al.*, 1998).

Brueckner & Medaris (2000) and Brueckner & Van Roermund (2004) proposed a similar tectonic scenario for the Scandian orogeny in the Caledonides. According to these authors, an intracontinental lithosphere-scale thrust fault formed after arc–Baltica collision (Brueckner & Medaris, 2000) or Laurentia-Baltica collision (Brueckner & Van Roermund, 2004) within the overridden continent (Baltica). The Western Gneiss region was buried to UHP depth in the footwall

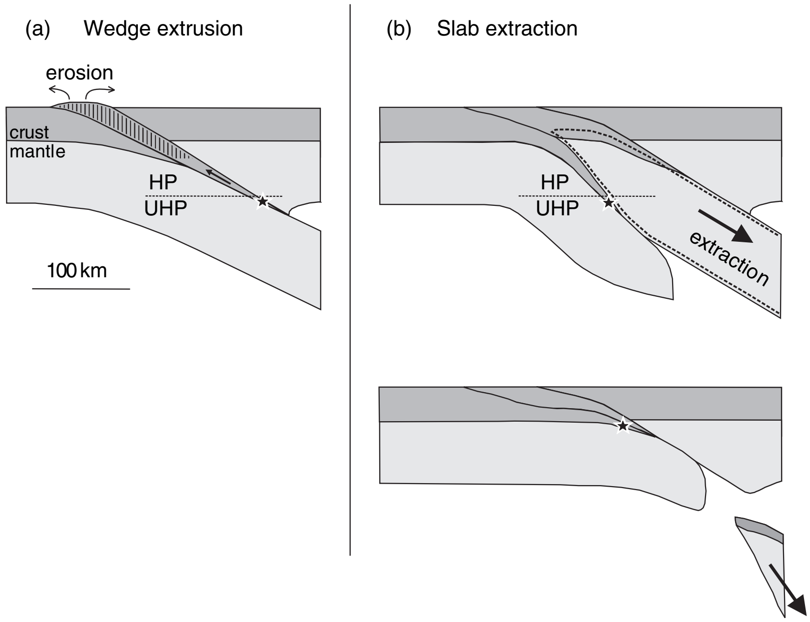

Fig. 9. Alternative models for UHP rock exhumation. (a) Wedge extrusion model. Exhumation of UHP rocks (star) to a depth near the base of normal continental crust implies the removal by erosion of the vertically ruled rock volume (cf. Chemenda *et al.*, 1995). (b) Slab extraction model (Froitzheim *et al.*, 2003) as proposed here for the exhumation of Pohorje UHP rocks. Above: before extraction; below: after extraction. Downward removal (subduction) of lower crustal and mantle wedge accommodates the same amount of exhumation as in 'A' without necessitating any erosion.

of this thrust fault. Whereas, in the case of the Western Gneiss Region, the evidence for such a scenario comes mostly from the geochemistry and geochronology of the garnet peridotites (see Brueckner & Medaris, 2000; Brueckner & Van Roermund, 2004), it is based on the large-scale geometry of the Austroalpine nappes in the case of the Eastern Alps (Janák *et al.*, 2004) and awaits the more geochemical and geochronological studies.

Exhumation of the Lower Central Austroalpine rocks was, for a large part, achieved by ductile deformation during the Late Cretaceous and was completed by brittle to ductile normal faulting in the Early to Middle Miocene (Fodor *et al.*, 2003). For the Late Cretaceous exhumation of the Lower Central Austroalpine HP rocks, recent publications have suggested a wedge-like extrusion, directed either towards the north (Tenczer & Stüwe, 2003) or towards the south (Sölva *et al.*, 2005). Irrespective of the direction of extrusion, the model requires erosion of large volumes of rocks with significant Cretaceous metamorphic fingerprints (Fig. 9a). However, there is no evidence in the Late Cretaceous sedimentary record of the Alps for these rocks (e.g. Bernoulli & Winkler, 1990; Von Eynatten & Gaupp, 1999). The intracontinental subduction scenario opens the possibility of slab extraction (Froitzheim *et al.*, 2003) as an alternative exhumation mechanism, that is, the downward removal (subduction) of the mantle and lower crustal wedge overlying the subducted Pohorje rocks (Fig. 9b). This mechanism allows considerable exhumation without the necessity of any significant erosion. In this case, the ultimate driving force of exhumation is not the buoyancy of the subducted continental crust – which is considerably reduced by the transition from quartz (density 2.65 g cm^{-3}) to coesite (density 3.01 g cm^{-3}) when the terrane enters UHP conditions – but the negative buoyancy of the extracted slab.

CONCLUSIONS

1 Garnet peridotites in the Pohorje Mountains record peak metamorphic conditions of 890–960 °C and 3.4–4 GPa, in the same range as peak conditions determined for the associated kyanite eclogites (Janák *et al.*, 2004). This confirms that the south-easternmost parts of the Austroalpine nappes in the Alps reached UHP metamorphic conditions during the Cretaceous orogeny. Garnet peridotites were subducted together with the eclogites to depths of at least 100 km.
2 Pohorje garnet peridotites have probably been derived from depleted mantle rocks, which were subsequently metasomatised by melts and/or fluids in the plagioclase-peridotite or the spinel-peridotite stability field. Subduction of these peridotite protoliths resulted in the development of garnet-bearing assemblages at HP and UHP conditions of metamorphism.
3 The proposed tectonic scenario is one where closure of the Meliata Ocean by continent–continent or arc–continent collision was followed by intracontinental subduction of the Pohorje nappe, belonging to the Lower Central Austroalpine, towards the SE under the Upper Central Austroalpine, which allowed subsequent exhumation of the UHP rocks by slab extraction.

ACKNOWLEDGEMENTS

We gratefully acknowledge H. Brueckner, R. Bousquet and J. Liou for their very helpful and constructive reviews and M. Brown for his editorial handling of this manuscript. We thank A. Hinterlechner-Ravnik for providing her material and help in the field. The Slovak Grant Agencies (grants APVT-20-020002 and VEGA 3167) and the Swedish Research Council (grant 621-2002-4282) supported this research.

REFERENCES

Altherr, R., Lugovic, B., Meyer, H. P. & Majer, V., 1995. Early Miocene post-collisional calc-alkaline magmatism along the easternmost segment of the periadriatic fault system (Slovenia and Croatia). *Mineralogy and Petrology*, **54,** 225–247.

Becker, H., 1993. Garnet peridotite and eclogite Sm-Nd mineral ages from the Lepontine dome (Swiss Alps): new evidence for Eocene high-pressure metamorphism in the central Alps. *Geology*, **21,** 599–602.

Becker, H., 1996. Crustal trace element and isotopic signatures in garnet pyroxenites and megacrysts from garnet peridotite massifs from Lower Austria. *Journal of Petrology*, **37,** 785–810.

Bernoulli, D. & Winkler, W., 1990. Heavy mineral assemblages from Upper Cretaceous South- and Austroalpine flysch sequences (northern Italy and southern Switzerland); source terranes and palaeotectonic implications. *Eclogae Geologicae Helvetiae*, **83,** 287–310.

Brenker, F. E. & Brey, G. P., 1997. Reconstruction of the exhumation path of the Alpe Arami garnet-peridotite body from depths exceeding 160 km. *Journal of Metamorphic Geology*, **15,** 581–592.

Brey, G. P. & Köhler, T., 1990. Geothermobarometry in four–phase lherzolites II. New thermobarometers, and practical assessment of existing thermobarometers. *Journal of Petrology*, **31,** 1353–1378.

Brueckner, H. K. & Medaris, L. G., 2000. A general model for the intrusion and evolution of 'mantle' garnet peridotites in high-pressure and ultra-high-pressure metamorphic terranes. *Journal of Metamorphic Geology*, **18,** 123–133.

Brueckner, H. K. & Van Roermund, H. L. M., 2004. Dunk tectonics: a multiple subduction/eduction model for the evolution of the Scandinavian Caledonides. *Tectonics*, **23,** TC2004, doi: 10.1029/2003TC001502.

Carswell, D. A. & Compagnoni, R., 2003. Introduction with review of the definition, distribution and geotectonic significance of ultrahigh pressure metamorphism. In: *Ultrahigh-pressure Metamorphism* (eds Carswell, D. A. & Compagnoni, R.), *EMU Notes in Mineralogy*, Vol. 5. pp. 3–9.

Carswell, D. A. & Van Roermund, H. L. M., 2005. On multiphase mineral inclusions associated with microdiamond formation in mantle-derived peridotite lens at Bardane on Fjortoft, west Norway. *European Journal of Minetralogy*, **17,** 31–42.

Chemenda, A. I., Mattauer, M., Malavieille, J. & Bokun, A. N., 1995. A mechanism for syn-collisional rock exhumation and associated normal faulting: results from physical modelling. *Earth and Planetary Science Letters*, **132,** 225–232.

Chopin, C., 2003. Ultrahigh-pressure metamorphism: tracing continental crust into the mantle. *Earth and Planetary Science Letters*, **212,** 1–14.

Desmurs, L., Müntener, O. & Manatschal, G., 2002. Onset of magmatic accretion within a magma-poor rifted margin: a case study from the Platta ocean-continent transition, eastern Switzerland. *Contributions to Mineralalogy and Petrology*, **144,** 365–382.

Dobrzhinetskaya, L. F., Green, H. W. & Wang, S., 1996. Alpe Arami: a Peridotite Massif from depths of more than 300 km. *Science*, **271,** 1841–1845.

Ernst, W. G., 1978. Petrochemical study of lherzolitic rocks from the Western Alps. *Journal of Petrology*, **19,** 341–392.

Fodor, L., Jelen, B., Márton, E. *et al*., 2002. Connection of Neogene basin formation, magmatism and cooling of metamorphics in NE Slovenia. *Geologica Carpathica*, **53** (Special Issue), 199–201.

Fodor, L., Balogh, K., Dunkl, I. *et al*., 2003. Structural evolution and exhumation of the Pohorje-Kozjak Mts., Slovenia. *Annales Universitatis Scientarum Budapestinensis, Sectio Geologica*, **35,** 118–119.

Froitzheim, N., Schmid, S. & Frey, M., 1996. Mesozoic paleography and the timing of eclogite-facies metamorphism in the Alps: a working hypothesis. *Eclogae Geologicae Helvetiae*, **89,** 81–110.

Froitzheim, N., Pleuger, J., Roller, S. & Nagel, T., 2003. Exhumation of high- and ultrahigh-pressure metamorphic rocks by slab extraction. *Geology*, **31,** 925–928.

Gebauer, D., 1996. A P-T-t path for an (ultra?) high pressure ultramafic/mafic rock-association and its felsic country-rocks based on SHRIMP-dating of magmatic and metamorphic zircon domains. Example: Alpe Arami (Central Swiss Alps). In: *Earth Processes: Reading the Isotopic Code* (eds Basu, A. & Hart, S.), *Geophysical Monograph, American Geophysical Union*, **95,** 307–329.

Godard, G., Martin, S., Prosser, G., Kienast, J. R. & Morten, L., 1996. Variscan migmatites, eclogites and garnet-peridotites of the Ulten zone, Eastern Austroalpine system. *Tectonophysics*, **259,** 313–341.

Harley, S. L., 1984. An experimental study of the partitioning of Fe and Mg between garnet and orthopyroxene. *Contributions to Mineralogy and Petrology*, **86,** 359–373.

Hinterlechner-Ravnik, A., 1987. Garnet peridotite from the Pohorje Mountains. *Geologija*, **30,** 149–181.

Hinterlechner-Ravnik, A., Sassi, F. P. & Visona, D., 1991. The Austridic eclogites, metabasites and metaultrabasites from the Pohorje area (Eastern Alps, Yugoslavia): 2. The metabasites and metaultrabasites, and concluding considerations. *Rendiconti Fisiche Accademia Lincei*, **2,** 175–190.

Hoinkes, G., Koller, F., Ranitsch, G. *et al*., 1999. Alpine metamorphism of the Eastern Alps. *Schweizerische Mineralogische und Petrographische Mitteilungen*, **79,** 155–181.

Holland, T. J. B. & Powell, R., 1998. An internally consistent thermodynamic data set for phases of petrological interest. *Journal of Metamorphic Geology*, **16,** 309–343.

Janák, M., Froitzheim, N., Lupták, B., Vrabec, M. & Krogh Ravna, E. J., 2004. First evidence for ultrahigh-pressure metamorphism of eclogites in Pohorje, Slovenia: tracing deep continental subduction in the Eastern Alps. *Tectonics*, **23,** TC5014, doi: 10.1029/2004TC001641.

Klemme, S., 2004. The influence of Cr on the garnet-spinel transition in the Earth's mantle: experiments in the system MgO-Cr_2O_3-SiO_2 and thermodynamic modelling. *Lithos*, **77,** 639–646.

Kretz, R., 1983. Symbols for rock-forming minerals. *American Mineralogist*, **68,** 277–279.

Krogh Ravna, E. J. & Paquin, J., 2003. Thermobarometric methodologies applicable to eclogites and garnet ultrabasites. In: *Ultrahigh-pressure Metamorphism* (eds Carswell, D. A. & Compagnoni, R.), *EMU Notes in Mineralogy*, **5,** 229–259.

Liati, A., Gebauer, D. & Fanning, C. M., 2003. The youngest basic oceanic magmatism in the Alps (Late Cretaceous; Chiavenna unit, Central Alps): geochronological constraints and geodynamic significance. *Contributions to Mineralogy and Petrology*, **146,** 144–158.

Liou, J. G., Zhang, R. Y., Ernst, W. G., Rumble, D. & Maruyama, S., 1998. High-pressure minerals from deeply subducted metamorphic rocks. In: *Ultrahigh-pressure Mineralogy: Physics and Chemistry of the Earth's Deep Interior* (ed. Hemley, R. J.), *Reviews in Mineralogy*, **37,** 33–96.

McDonough, W. F. & Sun, S., 1995. The composition of the Earth. *Chemical Geology*, **120,** 223–253.

Medaris, L. G. Jr, 2000. Garnet peridotites in Eurasian high-pressure and ultrahigh-pressure terranes: a discovery of origins and thermal histories. In: *UHP Metamorphism and geodynamics in Collision Type Orogenic Belts* (eds Ernst, W. G.

& Liou, J. G.), pp. 57–73. Geological Society of America, Boulder, CO.

Miller, C. & Thöni, M., 1997. Eo-Alpine eclogitisation of Permian MORB-type gabbros in the Koralpe (Eastern Alps, Austria): new geochronological, geochemical and petrological data. *Chemical Geology*, **137,** 283–310.

Miller, C., Mundil, R., Thöni, M. & Konzett, J., 2005. Refining the timing of eclogite metamorphism: a geochemical, petrological, Sm-Nd and U-Pb case study from the Pohorje Mountains, Slovenia (Eastern Alps). *Contributions to Mineralogy and Petrology*, **150,** 70–84.

Mioč, P. & Žnidarčič, M., 1977. Geological map of SFRJ 1:100 000, Sheet Slovenj Gradec. *Geological Survey, Ljubljana, Federal Geological Survey, Beograd.*

Müntener, O., Pettke, T., Desmurs, L., Meier, M. & Schaltegger, U., 2004. Refertilization of mantle peridotite in embryonic ocean basins: trace element and Nd isotopic evidence and implications for crust-mantle relationships. *Earth and Planetary Science Letters*, **221,** 293–308.

Neubauer, F. & Höck, V., 2000. Aspects of geology in Austria and adjoining areas: introduction. *Mitteilungen der Österreichischen Mineralogischen Gesellschaft*, **92,** 7–14.

Nimis, P. & Morten, L., 2000. P-T evolution of 'crustal'garnet peridotites and included pyroxenites from Nonsberg area (upper Austroalpine), NE Italy: from the wedge to the slab. *Journal of Geodynamics*, **30,** 93–115.

Nimis, P. & Trommsdorff, V., 2001. Revised thermobarometry of Alpe Arami and other garnet peridotites from the Central Alps. *Journal of Petrology*, **42,** 103–115.

O'Neill, H. StC. & Wood, B. J., 1979. An experimental study of Fe-Mg partitioning between garnet and olivine and its calibration as a geothermometer. *Contributions to Mineralogy and Petrology*, **70,** 59–70.

Obata, M. & Morten, L., 1987. Transformation of spinel lherzolite to garnet lherzolite in ultramatic lenses of the austridic crystalline complex, northern Italy. *Journal of Petrology*, **28,** 599–623.

Oberhänsli, R., Bousquet, R., Engi, M. *et al.*, (eds), 2004. Metamorphic structure of the Alps. *Mitteilungen der Österreichischen Mineralogischen Gesellschaft*, **149**.

Paquin, J. & Altherr, R., 2001. New constraints on the P-T evolution of the Alpe Arami garnet peridotite body (Central Alps, Switzerland). *Journal of Petrology*, **42,** 1119–1140.

Pearson, D. G., Davies, G. R. & Dixon, P. H., 1993. Geochemical constraints on the petrogenesis of diamond facies pyroxenites from the Beni Bousera peridotite massif, North Morocco. *Journal of Petrology*, **34,** 125–172.

Plašienka, D., 1995. Passive and active margin history of the northern Tatricum (Western Carpathians, Slovakia). *Geologische Rundschau*, **84,** 748–760.

Sassi, R., Mazzolli, C., Miller, C. & Konzett, J., 2004. Geochemistry and metamorphic evolution of the Pohorje Mountain eclogites from the easternmost Austroalpine basement of the Eastern Alps (Northern Slovenia). *Lithos*, **78,** 235–261.

Schmid, S. M., Fügenschuh, B., Kissling, E. & Schuster, R., 2004. Tectonic map and overall architecture of the Alpine orogen. *Eclogae Geologicae Helvetiae*, **97,** 93–117.

Schuster, R., Koller, F., Hoeck, V., Hoinkes, G. & Bousquet, R., 2004. Explanatory notes to the map: metamorphic structure of the Alps, Metamorphic evolution of the Eastern Alps. *Mitteilungen der Österreichischen Mineralogischen Gesellschaft*, **149,** 175–199.

Sölva, H., Grasemann, B., Thöni, M., Thiede, R. & Habler, G., 2005. The Schneeberg Normal Fault Zone: normal faulting associated with Cretaceous SE-directed extrusion in the Eastern Alps (Italy/Austria). *Tectonophysics*, **401,** 143–166.

Stampfli, G. M., Mosar, J., Marquer, D., Marchant, R., Baudin, T. & Borel, G., 1998. Subduction and obduction processes in the Swiss Alps. *Tectonophysics*, **296,** 159–204.

Tenczer, V. & Stüwe, K., 2003. The metamorphic field gradient in the eclogite type locality, Koralpe region, Eastern Alps. *Journal of Metamorphic Geology*, **21,** 377–393.

Thöni, M., 2002. Sm-Nd isotope systematics in garnet from different lithologies (Eastern Alps): age results, and an evaluation of potential problems for garnet Sm-Nd chronometry. *Chemical Geology*, **185,** 255–281.

Thöni, M. & Jagoutz, E., 1992. Some new aspects of dating eclogites in orogenic belts: Sm-Nd, Rb-Sr, and Pb-Pb isotopic results from the Austroalpine Saualpe and Koralpe type locality (Carinthia/Styria, southeastern Austria). *Geochimica et Cosmochimica Acta*, **56,** 347–368.

Thöni, M. & Miller, C., 1996. Garnet Sm-Nd data from the Saualpe and the Koralpe (Eastern Alps, Austria): chronological and P-T constraints on the thermal and tectonic history. *Journal of Metamorphic Geology*, **14,** 453–466.

Tumiati, S., Thöni, M., Nimis, P., Martin, S. & Mair, V., 2003. Mantle-crust interactions during Variscan subduction in the Eastern Alps (Nonsberg-Ulten zone): geochronology and new petrological constraints. *Earth and Planetary Science Letters*, **210,** 509–526.

Van Roermund, H. L. M. & Drury, M. R., 1998. Ultra-high pressure (P > 6 GPa) garnet peridotites in Western Norway: exhumation of mantle rocks from >185 km depth. *Terra Nova*, **10,** 295–301.

Visona, D., Hinterlechner-Ravnik, A. & Sassi, F. P., 1991. Geochemistry and crustal P-T polymetamorphic path of the mantle-derived rocks from the Pohorje area (Austrides, Eastern Alps, Slovenia). *Mineralia Slovaca*, **23,** 515–525.

Von Eynatten, H. & Gaupp, R., 1999. Provenance of Cretaceous synorogenic sandstones in the Eastern Alps; constraints from framework petrography, heavy mineral analysis and mineral chemistry. *Sedimentary Geology*, **124,** 81–111.

Webb, S. A. & Wood, B. J., 1986. Spinel-pyroxene-garnet relationships and their dependence on Cr/Al ratio. *Contributions to Mineralogy and Petrology*, **92,** 471–480.

Workman, R. K. & Hart, S. R., 2005. Major and trace element composition of the depleted MORB mantle (DMM). *Earth and Planetary Science Letters*, **231,** 53–72.

Zhang, R. Y. & Liou, J. G., 2003. Clinopyroxenite from the Sulu ultrahigh-pressure terrane, eastern China: origin and evolution of garnet exsolution in clinopyroxene. *American Mineralogist*, **88,** 1591–1600.

Zhang, R. Y., Liou, J. G. & Bolin, C., 1994. Petrogenesis of garnet-bearing ultramafic rocks and associated eclogites in the Su-Lu ultrahigh-P metamorphic terrane, eastern China. *Journal of Metamorphic Geology*, **12,** 169–186.

Received 12 May 2005; revision accepted 20 October 2005.